

2600, Australia.

¹M. L. Perl *et al.*, Phys. Rev. Lett. **35**, 1439 (1975).

²S. Y. Park and A. Yildiz, to be published; K. Fujikawa and N. Kawamoto, Phys. Rev. Lett. **35**, 1560 (1975); S. Y. Pi and A. I. Sanda, Phys. Rev. Lett. **36**, 1 (1976).

³E.g., from 8 to 24 extra fermions, not counting color multiplicity: M. Suzuki, Phys. Rev. Lett. **35**, 1553 (1975); L. Clavelli and A. Raychaudhuri, Phys. Rev. Lett. **35**, 1607 (1975). An infinite extension has also been contemplated: Z. Maki and I. Umemura, private communication. The smallest additions in the literature at the moment appear to be the following: H. Fritzsch, M. Gell-Mann, and P. Minkowski, Phys. Lett. **59B**, 256 (1975); cf. also R. L. Kingsley, F. Wilczek, and A. Zee, to be published; and also Z. Maki and I. Umemura, Prog. Theor. Phys. **53**, 1208 (1975), with two extra quarks and $2\frac{1}{2}$ extra leptons; Y. Achiman, K. Koller, and T. F. Walsh, Phys. Lett. **59B**, 261 (1975), with one extra quark and 2 to 4 extra leptons.

⁴Fritzsch, Gell-Mann, and Minkowski, Ref. 3; Kingsley, Wilczek, and Zee, Ref. 3; second reference to Maki and Umemura, Ref. 3.

⁵Achiman, Koller, and Walsh, Ref. 3.

⁶Take the mass of one charged heavy lepton to be that

suggested by the measurements of Ref. 1: about 1.8 GeV. For lack of further information, the other charged lepton may be taken several hundred MeV heavier, if we assume that mass differences rather than ratios are significant for the comparison between μ and e between strange and ordinary quarks. The neutral lepton masses are uncertain, one possibility being that they vanish.

⁷If the interaction is treated purely phenomenologically, the coupling constant for Eq. (3) can be $-G$, so the conventional magnitude is maintained.

⁸S. L. Glashow, J. Iliopoulos, and L. Maiani, Phys. Rev. D **2**, 1285 (1970).

⁹A. Benvenuti *et al.*, Phys. Rev. Lett. **35**, 1199, 1203, 1249 (1975), and earlier references cited there.

¹⁰S. Weinberg, Phys. Rev. Lett. **19**, 1264 (1969).

¹¹C. Bouchiat, J. Iliopoulos, and Ph. Meyer, Phys. Lett. **38B**, 519 (1972).

¹²Masses of all the gauge vectors seem to be in the usual ≥ 40 GeV range; special terms must be added only to remove the masslessness of the eight duplicate photons. Each Higgs scalar relates to its own set of gauge bosons in the usual way.

¹³Perhaps already observed by M. Cavalli-Sforza *et al.*, Phys. Rev. Lett. **36**, 558 (1976).

¹⁴J. W. Moffat, Phys. Rev. Lett. **35**, 1605 (1975).

Calculation of a Two-Electron-One-Photon Transition Rate for Fe^{\dagger}

Hugh P. Kelly

Department of Physics, University of Virginia, Charlottesville, Virginia 22901

(Received 23 February 1976)

The transition rate for a correlated two-electron jump into the doubly ionized K shell of Fe followed by emission of only one photon has been calculated using many-body perturbation theory. The ratio of the rate for the usual one-electron-one-photon transition to that of the two-electron-one-photon transition was calculated to be 0.563×10^4 in the length approximation and 0.586×10^4 in the velocity approximation. These results compare favorably with the ratio of $(0.4 \pm 0.3) \times 10^4$ measured recently by Wölfli *et al.*

In a recent Letter by Wölfli, Stoller, Bonani, Suter, and Stöckli,¹ results were given for the interesting process of a two-electron jump into the doubly ionized K shells of Ni and Fe followed by the emission of only one photon carrying away the total transition energy. This effect was observed during an investigation of the noncharacteristic part of the x-ray spectra produced in Ni-Ni, Ni-Fe, Fe-Ni, and Fe-Fe collisions. Momentum-analyzed beams of $^{58}\text{Ni}^{6+}$ and $^{56}\text{Fe}^{6+}$ were used to induce the x rays in ^{58}Ni (1 mg/cm²) and thick natural-Fe targets.

Although this effect was predicted years ago by Heisenberg,² Condon,³ and Goudsmit and Groppe,⁴ it had not been observed until the recent work by Wölfli *et al.*¹ Also, there do not appear to exist any calculations of this effect which in-

volve electron correlations. In this paper results are presented for the rate of two-electron-one-photon jumps into the doubly ionized K shell of Fe. Many-body perturbation theory⁵⁻⁷ was used to calculate the correlated wave functions starting from a Hartree-Fock (HF) expression as the lowest-order function. All terms were included which correspond to first-order correlation corrections in either the initial state or the final state. The radiative matrix elements which are required are $\langle \psi_f | \sum_j \vec{r}_j | \psi_i \rangle$, where $|\psi_i\rangle$ is the correlated initial state of Fe^{++} with the doubly ionized K shell and configuration $2s^2 2p^6 2s^2 3p^6 3d^6 4s^2$. For the final state $|\psi_f\rangle$ the configuration $1s^2 2s 2p^5(^1P) 3s^2 3p^6 3d^6 - 4s^2$ was used. The dipole approximation is used here, but in a more accurate calculation one would not be restricted to this approximation.

Since the $2s2p - 1s^2$ transition is being calculated, the details of the configuration of the outer electrons should not be significant and the calculated results may be compared with the experiment which involved Fe^{6+} beams and thick natural-Fe targets.

Diagrams representing the terms in the perturbation expansion are shown in Fig. 1. Since $|\psi_f\rangle$ is represented by a linear combination of determinants, one must use projections⁸ in obtaining the angular factors from the diagrams. Rayleigh-Schrödinger perturbation theory may also be used to calculate the angular coefficients. The diagrams proceed from bottom to top corresponding to right to left in $\langle\psi_f|\sum_j \vec{r}_j|\psi_i\rangle$. The dashed line between two solid lines represents Coulomb interactions, and the dashed line terminating in a solid circle represents interaction with the radiation field. In the present case this is taken to be $\sum_i \vec{r}_i$ or the corresponding velocity form.⁹ In the diagrams, Coulomb interactions above and below the dipole interaction represent correlations in $|\psi_f\rangle$ and $|\psi_i\rangle$, respectively.¹⁰ Denominators occurring after the dipole interaction are shifted by $-\omega$ corresponding to the energy of the outgoing photon and so become the appropriate

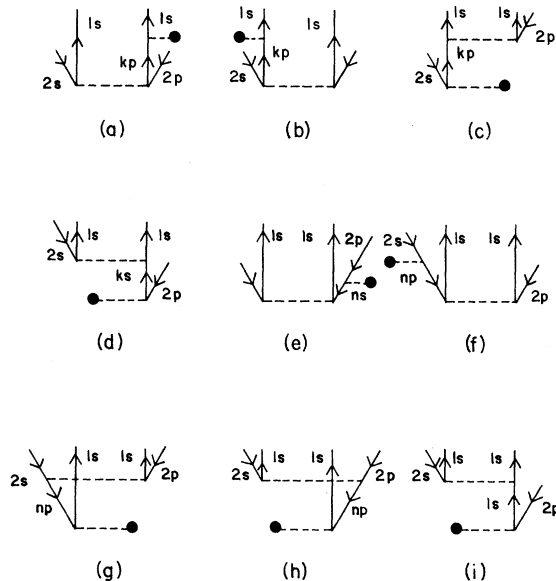


FIG. 1. Diagrams contributing to the two-electron one-photon radiative matrix element $\langle\psi_f|\sum_j \vec{r}_j|\psi_i\rangle$ for the $2s2p \rightarrow (1s)^2$ transition. Dashed lines terminating in solid circles represent matrix elements of \vec{r} . Other dashed lines represent Coulomb interactions. ns and np represent hole states $2s, 3s, 4s$, and $2p, 3p$, respectively. The symbols ks and kp represent sums over bound and continuum excited states with $l=0$ and $l=1$, respectively.

denominators for $|\psi_f\rangle$. In diagrams (a) and (b) the denominators vanish for $\epsilon_{2s} + \epsilon_{2p} - \epsilon_{1s} - \epsilon_{kp} = 0$ and this singularity is treated by adding $+i\eta$ to the denominator.¹¹ These diagrams then have both real and imaginary parts, with the imaginary part related to the Auger process.¹¹

The diagrams were evaluated numerically by the methods of Ref. 7, and the results are given in Table I. Diagrams (h) (with $np = 2p$) and (i) account for the nonorthogonality of P_{2s} in $|\psi_i\rangle$ with P_{1s} in $|\psi_f\rangle$ and can be calculated by separate Hartree-Fock calculations for $|\psi_i\rangle$ and $|\psi_f\rangle$. Although this effect is important, the other diagrams which involve correlations are also important and must be included to obtain an accurate result. These calculations were carried out non-relativistically and used the Hartree-Fock program of Fischer¹² to obtain the initial HF approximation to $|\psi_i\rangle$ and $|\psi_f\rangle$. The calculated value for $\omega = E_i - E_f$ is 471.96 a.u. or 12.843 keV as compared with 13.048 keV measured by Wölfli *et al.*¹

Using the results of Table I, the two-electron one-photon transition rate for $2s2p - (1s)^2$ is 6.270×10^{-6} a.u. in the length approximation and 5.432×10^{-6} a.u. in the velocity approximation. The rate for one-electron one-photon decay $2s^22p^6 \rightarrow 1s2s^22p^5$ is 3.532×10^{-2} a.u. in the length approximation and 3.167×10^{-2} a.u. in the velocity approximation. The ratio of the one-electron one-photon rate to the two-electron one-photon rate is then 0.563×10^4 in the length approximation and 0.586×10^4 in the velocity approximation.

TABLE I. Contributions of the diagrams of Fig. 1 to $\langle\psi_f|\sum_j \vec{r}_j|\psi_i\rangle$.^a

Diagram	Length form (a.u.)	Velocity form (a.u.)
a	5.556×10^{-5}	1.100×10^{-2}
	$-i7.475 \times 10^{-5}$	$-i3.601 \times 10^{-2}$
b	-8.035×10^{-6}	-9.300×10^{-3}
	$-i4.370 \times 10^{-5}$	$-i2.106 \times 10^{-2}$
c	-1.041×10^{-4}	1.268×10^{-2}
d	-4.297×10^{-5}	4.045×10^{-3}
e	2.105×10^{-5}	1.108×10^{-3}
f	1.482×10^{-4}	2.269×10^{-4}
g	-6.446×10^{-5}	-1.484×10^{-2}
h	3.166×10^{-5}	7.393×10^{-3}
i	-4.350×10^{-4}	-1.009×10^{-1}
Total	-2.086×10^{-4}	-8.859×10^{-2}
	$-i1.185 \times 10^{-4}$	$-i5.707 \times 10^{-2}$

^aFactor $\sqrt{2}$ due to $2s2p^5(^1P)$ coupling in $|\psi_f\rangle$ is not included. Also, the angular factor for the dipole interaction is not included.

These values are in reasonable agreement with the value $(0.4 \pm 0.3) \times 10^4$ measured for Fe by Wölfli *et al.*¹

It should be noted that the calculation is somewhat idealized because it was carried out assuming an initial state with two 1s vacancies but no vacancies in the *L* shell. It is likely that there will be a distribution of vacancies in the *L* shell¹³ and that there will be a resulting decrease in both the two-electron-one-photon and one-electron-one-photon rates. However, it is expected that the ratio of these rates will in general change more slowly with vacancies than either rate alone. The atom can, of course, also undergo two-electron-one-photon decays with the transitions $2s3p \rightarrow (1s)^2$, $3s2p \rightarrow (1s)^2$, etc. Although these rates were not explicitly calculated, a number of the appropriate matrix elements were obtained and it is estimated that the $2s3p$ and $3s2p$ rates are 5 to 10 times smaller than the $2s2p \rightarrow (1s)^2$ rate. It would also be interesting to include relativistic effects and all multipole radiation.

I wish to thank Professor W. Mehlhorn for bringing this work to my attention and Professor R. McKnight for helpful discussions. I am also

grateful to Professor C. Froese Fischer for the generous use of her computer program.

[†]Work supported by the National Science Foundation.

¹W. Wölfli, Ch. Stoller, G. Bonani, M. Suter, and M. Stöckli, *Phys. Rev. Lett.* **35**, 656 (1975).

²W. Heisenberg, *Z. Phys.* **32**, 841 (1925).

³E. U. Condon, *Phys. Rev.* **36**, 1121 (1930).

⁴S. Goudsmit and L. Gropper, *Phys. Rev.* **38**, 225 (1931).

⁵K. A. Brueckner, *Phys. Rev.* **97**, 1353 (1955), and *The Many-Body Problem* (Wiley, New York, 1959).

⁶J. Goldstone, *Proc. Roy. Soc. London, Ser. A* **239**, 267 (1957).

⁷H. P. Kelly, *Adv. Theor. Phys.* **2**, 75 (1968).

⁸S. L. Carter and H. P. Kelly, to be published.

⁹H. A. Bethe and E. E. Salpeter, *Quantum Mechanics of One- and Two-Electron Atoms* (Springer, Berlin, 1957).

¹⁰H. P. Kelly and R. L. Simons, *Phys. Rev. Lett.* **30**, 529 (1973).

¹¹R. L. Chase, H. P. Kelly, and H. S. Köhler, *Phys. Rev. A* **3**, 1550 (1971).

¹²C. Froese Fischer, *Comput. Phys. Commun.* **1**, 151 (1969).

¹³F. Jundt and D. J. Nagel, *Phys. Lett.* **50A**, 179 (1974).

Orbital Waves in ³He-A at Zero Temperature

M. Combescot and R. Combescot

Groupe de Physique des Solides de l'École Normale Supérieure, 75231 Paris Cedex 05, France

(Received 7 April 1976)

At zero temperature, orbital waves propagate in ³He-A with a dispersion relation $\omega = q_{\#} v_F$ in the regime $T_c^2/E_F \ll \hbar\omega \ll T_c$; the damping is also studied. In the regime $\hbar\omega \ll T_c^2/E_F$, undamped orbital waves propagate with the dispersion relation $\omega \sim (E_F/T_c^2)(q_{\#} v_F)^2 \ln(T_c/q_{\#} v_F)$.

Orbital waves are the Goldstone modes of the *A* phase of superfluid ³He associated with the degeneracy with respect to the rotation of the anisotropy axis \hat{l} . In a recent Letter,¹ orbital waves in ³He-A have been shown to be diffusive at finite temperature, in the collisionless regime as well as in the hydrodynamic regime. This overdamping is due to the fact that, when \hat{l} is moving, the quasiparticle distribution has to be modified, even in the limit $\omega \rightarrow 0$. Therefore, in the motion \hat{l} is dragging along quasiparticles, that is, the normal fluid, which produces the damping.

Since the overdamping is linked to thermally excited quasiparticles, one may expect that orbital

waves propagate at $T = 0$ where there are no longer quasiparticles. Here we want to complete our former kinetic-equation analysis in the collisionless regime to include the $T = 0$ limit which was not considered in Ref. 1. We find indeed that orbital waves propagate at $T = 0$ with various dispersion relations depending on the frequency regime. These results should hold at finite temperature, as long as $kT \ll \hbar\omega, qv_F$, whereas the overdamped regime found in Ref. 1 corresponds to $kT \gg \hbar\omega, qv_F$. The transition from one regime to the other occurs for $\hbar\omega, qv_F \sim kT$.

Let us first note that the collisionless regime is likely to be the only physical one at low tem-